

Letter

# Manual-Based Improvement Method for the ASTER Global Water Body Data Base

Hiroyuki Fujisada <sup>1,\*</sup>, Minoru Urai <sup>1,2</sup> and Akira Iwasaki <sup>1,3</sup> 

<sup>1</sup> Sensor Information Laboratory Corp., 2-23-36 Shihaugaoka, Tsukubamirai, Ibaraki 300-2359, Japan; urai-minoru@aist.go.jp (M.U.); aiwasaki2@g.ecc.u-tokyo.ac.jp (A.I.)

<sup>2</sup> Institute of Advanced Industrial Science and Technology (AIST), 1-1-1, Higashi, Tsukuba, Ibaraki 302-8564, Japan

<sup>3</sup> Department of Aeronautics and Astronautics, University of Tokyo, Tokyo 113-8656, Japan

\* Correspondence: fujisada@silc.co.jp; Tel.: +81-297-21-7244

Received: 2 September 2020; Accepted: 9 October 2020; Published: 15 October 2020



**Abstract:** A water body detection technique is an essential part of digital elevation model (DEM) generation to delineate land–water boundaries and to set flattened elevations. The initial tile-based water body data that are created during production of the Advanced Spaceborne Thermal Emission and Reflection radiometer (ASTER) GDEM, as a by-product, are incorporated into ASTER GDEM V3 to improve the quality. At the same time as ASTER GDEM V3, the Global Water Body Data Base (ASTWBD) Version 1 is also released to the public. The ASTWBD generation consists of two parts: separation from land area, and classification into three categories: sea, lake, and river. Sea water bodies have zero elevation. Lake water bodies have flattened elevations. River water bodies have a gradual step-down from upstream to downstream with a step of one meter. The separation process from land area is carried out automatically using an algorithm, except for sea-ice removal, to delineate the real seashore lines in the high latitude areas; almost all of the water bodies are created through this process. The classification process into three categories, i.e., sea, river, and lake, is carried out, and incorporated into ASTER GDEM V3. For inland water bodies, it is not possible to perfectly detect all water bodies using reflectance and spectral index, which are the only available parameters for optical sensors. The only way available to identify the undetected inland water bodies is to manually copy them with visual inspection from the earth’s surface images, like Landsat images. GeoCover2000 images are the main part of the object images. Color–Land ASTER MosaicS (CLAMS) images are used to cover the deficiency of the GeoCover2000 images. This kind of time-consuming, unsophisticated way is inevitable as it is a manual-based method to improve the quality of the ASTWBD. This paper describes the manual-based improvement method; specifically, how deficient water body images are efficiently copied as rasterized images from the earth’s surface images to obtain a more complete global water body data set.

**Keywords:** ASTER; optical sensor; digital elevation model; global data base; water body data base

## 1. Introduction

The Advanced Spaceborne Thermal Emission and Reflection radiometer (ASTER) is an advanced multispectral imaging sensor that was launched on board the Terra spacecraft in December, 1999 [1,2]. ASTER mosaics consist of band 3N as red and band 2 as green. ASTER has an along-track stereoscopic viewing capability in its visible and near-infrared (VNIR) bands at a 15-m spatial resolution with a base-to-height ratio of 0.6. Because of ASTER’s excellent satellite ephemeris and instrument parameters, this along-track stereoscopic viewing capability makes it possible to generate excellent digital elevation

model (DEM) data products from ASTER data without referring to ground control points (GCPs) for individual scenes [3–5].

Water body detection is an essential part of DEM generation, because image matching is not possible for water bodies. The Global Water Body Data Base (ASTWBD) generation consists of two parts: (1) separation of water bodies from land area, including separation of sea area; and (2) classification of two inland water bodies, i.e., lakes and rivers. The separation process (1) was generated automatically using an algorithm, except for sea-ice removal, to delineate the real seashore lines in the high latitude areas and incorporated into the ASTER GDEM V3 to improve the quality. Almost all the water bodies were created through this process. However, the existence of inland water bodies missed by this automatic process must be kept in mind, as shown later. The separation process (2) was manually carried out with visual inspection (see reference [6] for details). For inland water bodies like lakes and rivers, it is not possible to perfectly detect all water bodies using reflectance and spectral index, which are the only available parameters for optical sensors like ASTER. The only way available to identify the missed inland water bodies is to manually copy them with time-consuming visual inspection from the earth's surface images, like Landsat images. GeoCover2000 [7] images are a main part of the reference images. GeoCover2000 is used in this paper. Color-Land ASTER MosaicS (CLAMS) [8] images are used to cover the deficiency of the GeoCover images. The original GeoCover data set covers the earth with a 14.25 m spatial resolution and UTM coordinate. The original CLAMS data set covers the earth every 4° latitude by 4° longitude with 0.5 arcsecond posting. Both data sets were converted to the same spatial resolution and coordinates as the ASTER GWBD, i.e., geographic latitude/longitude coordinates with 1 arcsecond posting, and a 1° latitude by 1° longitude tile size. Each ASTER GWBD folder is composed of an attribute file and a DEM file. The attribute file distinguishes a type of water body: a sea water body (Attribute 1), river water body (Attribute 2), and lake water body (Attribute 3). The attribute types are usually depicted with color density slice images in this paper. Attributes 1, 2, and 3 are depicted with blue, red, and green colors, respectively.

The improvement work was accomplished using the support tool that utilizes the “Region of Interest” (ROI) and “Masking” functions of “ENVI” image analysis software by Harris Geospatial Solutions. The support tool “ROI” was used to copy the missed inland water bodies on either object image. Then, the support tool “Masking” was used to import the copied images to the water body image tile, and the improved image tile was saved as a GeoTIFF file.

## 2. Improvement by GeoCover or CLAMS Images

### 2.1. Features of the GeoCover and CLAMS Images

GeoCover is a false-color composite image created from orthorectified Landsat Enhanced Thematic Mapper (ETM+) mosaics of band 7 as red, band 4 as green, and band 2 as blue [9,10]. CLAMS is a pseudo-true color composite image created from ASTER mosaics of band 3N as red, band 2 as green, and simulated blue as blue. The simulated blue is used, since ASTER lacks a blue band (see reference [8] for more details about the simulated blue).

Figure 1 shows the relation between the two reference images and corresponding water body image. The water bodies are shown as green density slice image. In the GeoCover images, water body areas almost accurately correspond to the black and dense-blue color areas. On the other hand, in the CLAMS images, water body areas are widely spreaded from black to white color areas, and then careful judgement will be required.

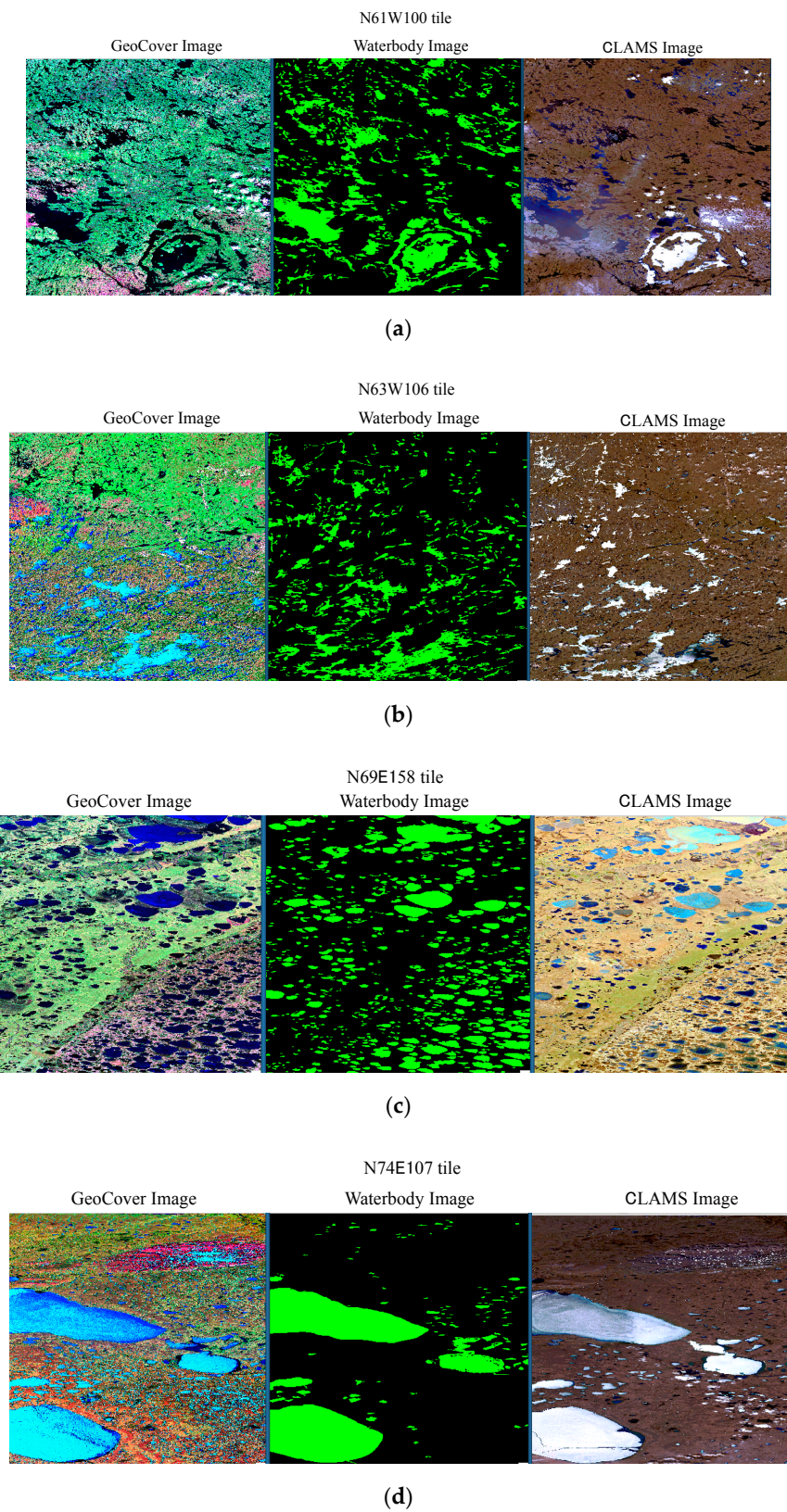


**Figure 1.** Typical examples of GeoCover and CLAMS images to grasp the feature for water bodies. The corresponding water body are shown as green density slice images. Tile size: 1° latitude by 1° longitude: (a) Images of the N61W100 tiles; (b) Images of the N63W106 tiles; (c) Images of the N69E158 tiles; (d) Images of the N74E107 tile.

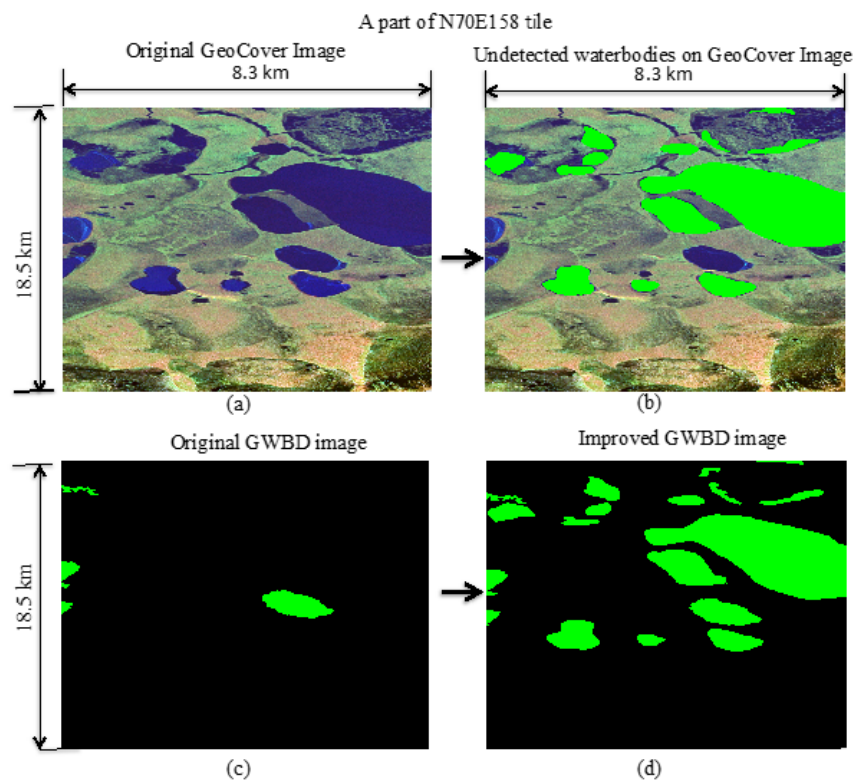
## 2.2. How the Improved ASTWBD Was Created

Figure 2 show the water body improvement process using a GeoCover image as the reference image. Each image is a part of the N70E158 tile with an 800-by-600-pixel sub-area that correspond to 8.3 km by 18.5 km, because one arcsecond corresponds to 30.8 m at the equator. The improvement process was carried out as follows:

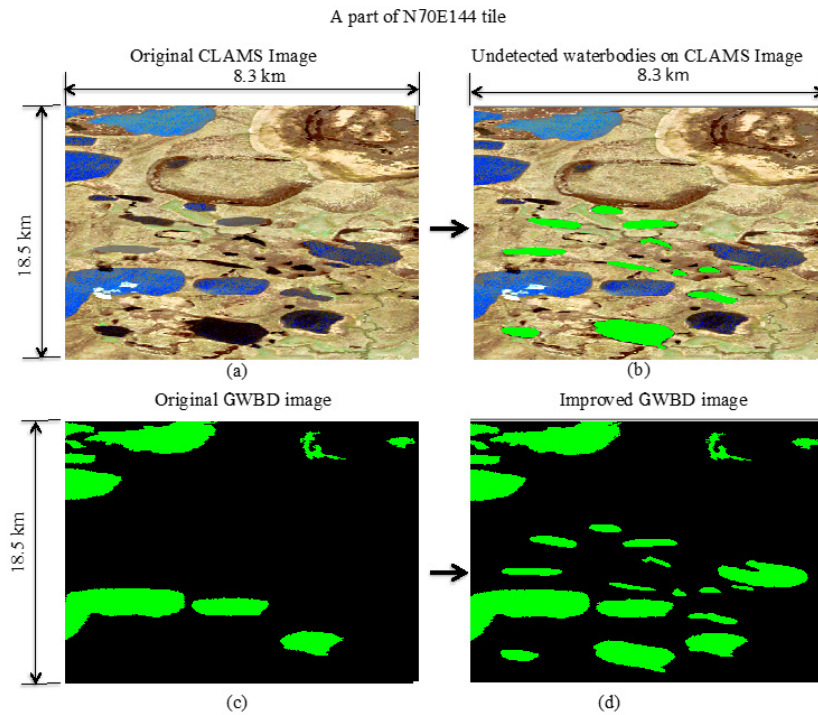
- (1) Compare the original GWBD image (Figure 2c) before correction with the reference images (Figure 2a) to find the undetected water body areas.
- (2) The undetected water body areas are filled in green on the GeoCover image as shown in Figure 2b using the support tool “ROI”. The green color areas correspond to the undetected areas.
- (3) The undetected areas on the GeoCover image are imported to the GWBD image and saved as a GeoTIFF file using the support tool “Masking” function.
- (4) The final improved GWBD image is shown in Figure 2d.

Figure 3 shows the water body improvement process using the CLAMS image as the reference image. The water body improvement process using the CLAMS image is the same as the case of the GeoCover image, as shown above. The GeoCover image is more excellent than the CLAMS image, as shown in the previous section, and so the GeoCover images are used as the main part of the reference images. CLAMS images are used only if the GeoCover image file does not exist.

The water body improvement process is carried out mainly in the area of 60 degrees north and further north latitude, since the Shuttle Radar Topography Mission (SRTM) Water Body Data product (SWBD) [9] is available to make up the undetected water body areas between south 56 degrees and north 60 degrees. South of south 56 degrees areas are not important for inland water bodies because of the frozen Antarctica.



**Figure 2.** The improvement process of undetected water body areas using a GeoCover image as the reference: (a) original GeoCover image; (b) undetected water body areas filled with green on original the GeoCover image; (c) original GWBD image; (d) improved GWBD image. The GWBD images are shown as green density slice images.



**Figure 3.** The improvement process of undetected water body areas using a CLAMS image as the reference: (a) original CLAMS image; (b) undetected water body areas filled with green on the original CLAMS image; (c) original GWBD image; (d) improved GWBD image. The GWBD images are shown as green density slice images.

### 2.3. Typical Examples of Improvements

Figure 4 shows four typical examples of the improvement using GeoCover images or CLAMS images. The image tiles with large, increased occupancy ratios were selected as the typical examples. Although the improvements are mainly carried out by GeoCover reference images, it is shown that the CLAMS reference images also play an important role in perfect improvement by covering the deficiencies of the GeoCover images. Figure 4c,d specifically point out that not only small lakes but also large ones are added as water bodies by the CLAMS reference images.

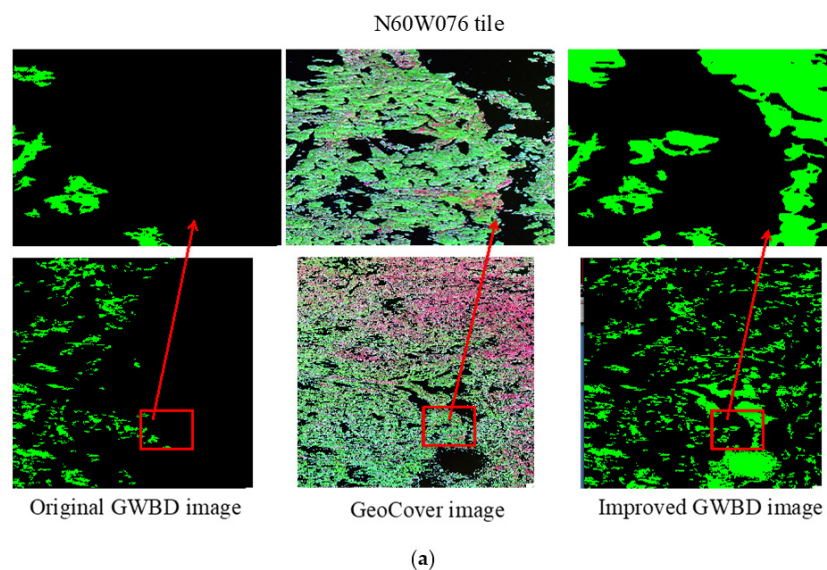


**Figure 4.** Cont.

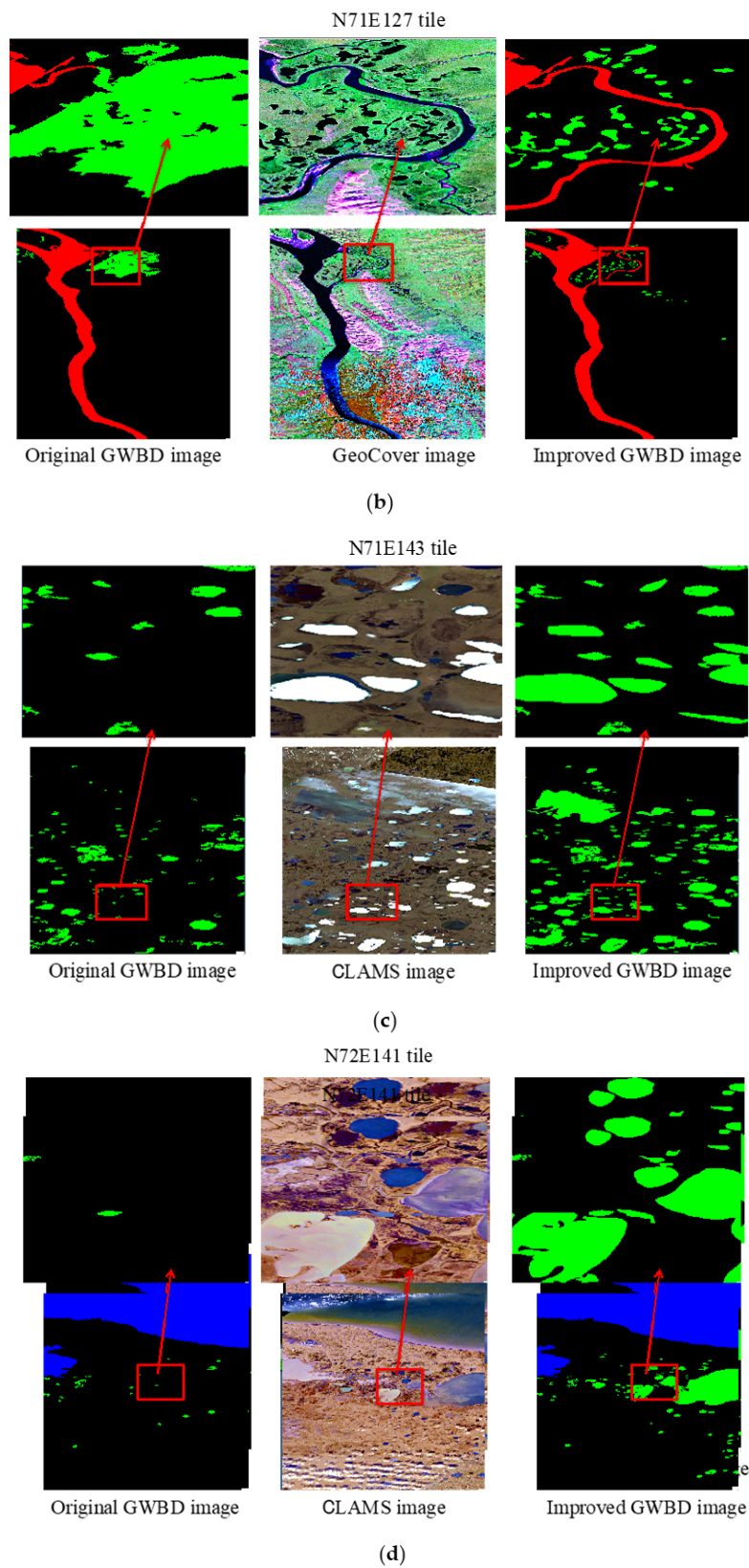


**Figure 4.** Four typical examples of improvement using GeoCover images (a,b) or CLAMS images (c,d). For each example, the lower and the upper images show the entire tile images and partially expanded sub-area images with 600 by 400 pixels, respectively. The expanded sub-area in each entire tile image is shown by the rectangular red line. Tile size: 1° latitude by 1° longitude: (a) Images of the N60W076 tiles; (b) Images of the N71E127 tiles; (c) Images of the N71E143 tiles; (d) Images of the N72E141 tiles.

More detailed quantitative water body occupancy data are shown in Table 1. Table 2 shows the area list for the large increased occupancy ratios of the lake-type water bodies in ascending order, starting from 0.52127% to a final maximum value of 33.45049%.

**Table 1.** Detailed quantitative water body occupancy data for the four typical examples shown in Figure 4.

Tile Name	Type of Images	Sea Occupancy (%)	River Occupancy (%)	Lake Occupancy (%)
N60W076	Original image	0	0	6.56163
	Improved image	0	0	18.36819
N71E127	Original image	0	8.55893	2.52542
	Improved image	0	8.81181	0.60127
N71E143	Original image	0	0	4.83586
	Improved image	0	0	14.03497
N72E141	Original image	22.28395	0	0.38985
	Improved image	22.28395	0	6.48122

**Table 2.** Increased occupancy ratios of the lake-type water bodies in ascending order to the high-ratio areas. The ratios are shown with the corresponding tiles and locations.

Tile Name	Location	Ratio (%)	Tile Name	Location	Ratio (%)	Tile Name	Location	Ratio (%)
N60E007	Norway	5.25127	N64W095	Canada	6.79022	N68W097	Canada	9.95321
N61W098	Canada	5.28094	N68E145	Russia	6.81613	N71W109	Canada	10.13983
N71E141	Russia	5.33550	N65W097	Canada	6.87522	N69W105	Canada	10.19871
N72E097	Russia	5.39406	N70W112	Canada	6.91013	N61W164	USA (Alaska)	10.24639
N60W100	Canada	5.40833	N71W111	Canada	6.91214	N70W111	Canada	10.55154
N75E112	Russia	5.41753	N69W125	Canada	6.92857	N65W114	Canada	10.56258
N72E142	Russia	5.45569	N63W099	Canada	7.04038	N66W098	Canada	10.64937
N71E080	Russia	5.46514	N68W090	Canada	7.06019	N70W157	USA (Alaska)	10.67472
N66W105	Canada	5.50322	N71E140	Russia	7.16263	N63W106	Canada	10.79045
N70E078	Russia	5.52684	N64W098	Canada	7.19305	N70W154	USA (Alaska)	10.94286
N69W098	Canada	5.54657	N61W165	USA (Alaska)	7.28413	N64W114	Canada	10.95453
N67W115	Canada	5.56222	N62W108	Canada	7.32367	N63W097	Canada	11.10577
N72W108	Canada	5.59931	N63W118	Canada	7.38103	N60W164	USA (Alaska)	11.20842
N60W074	Canada	5.62596	N61W099	Canada	7.43363	N70E158	USA (Alaska)	11.25973
N63W095	Canada	5.63278	N67W126	Canada	7.62890	N62W102	Canada	11.31035
N60W165	Russia	5.63698	N64W115	Canada	7.73903	N62W101	Canada	11.33130
N65W105	Canada	5.65309	N71E096	Russia	7.76664	N62W096	Canada	11.36850
N61E008	Norway	5.67248	N63W110	Canada	7.83731	N64W108	N64W108	11.47643
N69W104	Canada	5.71586	N62W109	Canada	7.95232	N64W117	N64W117	11.49349
N69E124	Russia	5.76290	N70W105	Canada	7.97608	N68E154	N68E154	11.64781
N65W108	Canada	5.85980	N62W104	Canada	8.03119	N60W076	N60W076	11.80715
N70E079	Russia	5.87961	N69E156	Russia	8.08248	N70W156	N70W156	12.06289
N71E095	Russia	5.94174	N70E159	Russia	8.08720	N65W099	N65W099	12.13787
N61W075	Canada	5.94803	N68W128	Canada	8.10427	N69W113	N69W113	12.33947
N64W093	Canada	5.94889	N63W096	Canada	8.13296	N65W116	N65W116	12.63866
N70W106	Canada	5.95411	N61W096	Canada	8.14558	N63W109	N63W109	12.69144
N70W088	Canada	6.00687	N65W115	Canada	8.22398	N65W113	N65W113	12.88074
N70E150	Russia	6.02750	N64W113	Canada	8.25485	N65W117	N65W117	13.15168
N72E141	Russia	6.09137	N67W105	Canada	8.51486	N66W104	N66W104	13.47813
N63W094	Canada	6.09459	N69E155	Russia	8.53566	N72W107	N72W107	13.65664
N70E153	Russia	6.18505	N72W106	Canada	8.75356	N61W111	N61W111	14.22826
N61W139	Canada	6.22052	N70W110	Canada	8.80408	N61W101	N61W101	14.36880
N64E029	Finland	6.25783	N68E071	Russia	8.83583	N62W095	N62W095	14.62151
N65W104	Canada	6.27058	N68W133	Canada	8.96451	N61W104	Canada	14.89520
N71W110	Canada	6.35164	N67W107	Canada	8.98649	N69W112	Canada	15.19103
N64W096	Canada	6.41225	N70W155	USA (Alaska)	9.00188	N64W118	Canada	15.41963
N61W095	Canada	6.44154	N68E155	Russia	9.02434	N62W100	Canada	15.48538

Table 2. Cont.

Tile Name	Location	Ratio (%)	Tile Name	Location	Ratio (%)	Tile Name	Location	Ratio (%)
N67W102	Canada	6.48683	N70W153	USA (Alaska)	9.09714	N65W100	Canada	15.50255
N63W101	Canada	6.52677	N67W104	Canada	9.14772	N62W103	Canada	15.55613
N69W111	Canada	6.57954	N68E070	Russia	9.19645	N66W103	Canada	16.04481
N70W113	Canada	6.58299	N71E143	Russia	9.19910	N61W100	Canada	16.81194
N64W109	Canada	6.59901	N65W111	Canada	9.23940	N61W103	Canada	17.00779
N67W098	Canada	6.65046	N74E107	Russia	9.33596	N63W107	Canada	17.57145
N65W098	Canada	6.65231	N69E159	Russia	9.40438	N66W099	Canada	17.66327
N70W158	USA (Alaska)	6.69218	N69E158	Russia	9.52341	N60W075	Canada	18.45545
N69E146	USA (Alaska)	6.70507	N64W107	Canada	9.61353	N63W108	Canada	18.94309
N66W115	Canada	6.70820	N67W106	Canada	9.67472	N62W107	Canada	21.11334
N65W157	USA (Alaska)	6.74008	N67W103	Canada	9.82968	N75E142	Russia	33.45049

### 3. Discussion

The ASTWBD plays a very important role in the ASTER GDEM generation process, because image matching is not possible for water bodies and is directly linked to ASTER GDEM quality. The special feature of a water body is its flattened elevation value for seas and lakes, and a step-down elevation value from upstream to downstream for rivers. The improved GWBD must be incorporated into the corresponding GDEM image to reflect the improvement effects. Figure 5 shows the effects of the improved GWBD images to the corresponding GDEM images. The image areas are the same as the expanded sub-area of the typical examples shown in Figure 4. Two lower images are the original and improved color density slice GWBD images. A green color denotes a lake water body. The two upper images correspond to the original and improved shaded-relief GDEM images, in which the water bodies are flattened, and clearly show the effect of GWBD improvement on ASTER GDEM quality.

Figure 6 shows the GWBD improvement effects by color density slice occupancy ratio images for inland water bodies on a global scale. Large yellow-color areas denote sea areas. The inland water body means lakes and rivers. In Figure 6a,b, the color density slice images illustrate a red-type color when the occupancy ratios are larger than about 50%, and green- or blue-type colors when the occupancy ratios are smaller than about 50%. On the other hand, in Figure 6c, the color density slice images illustrate a red-type color when the increased occupancy ratios are larger than about 15%, and green- or blue-type colors when the increased occupancy ratios are smaller than about 15%, since the maximum is 33.45%, as shown in Table 2

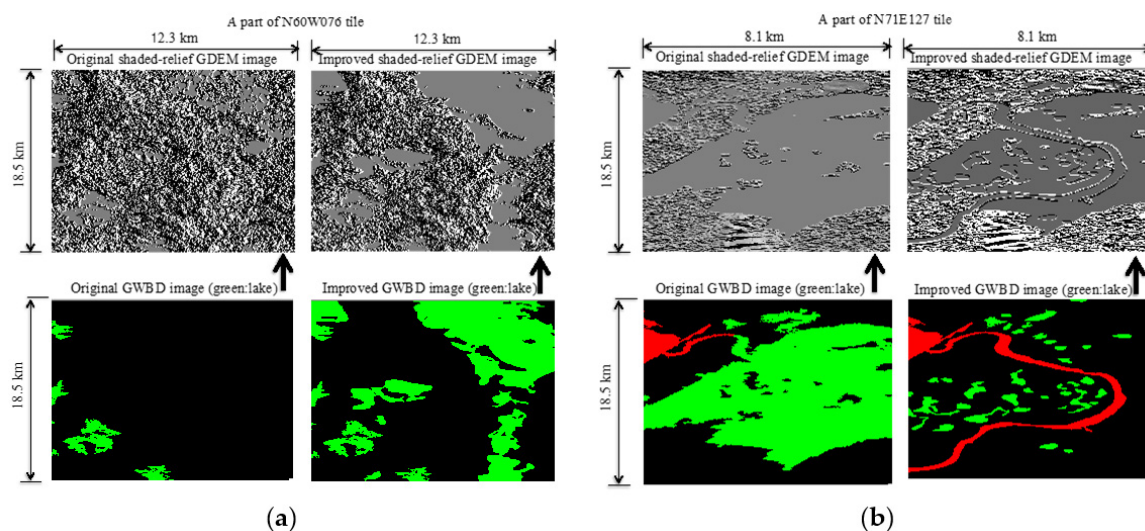
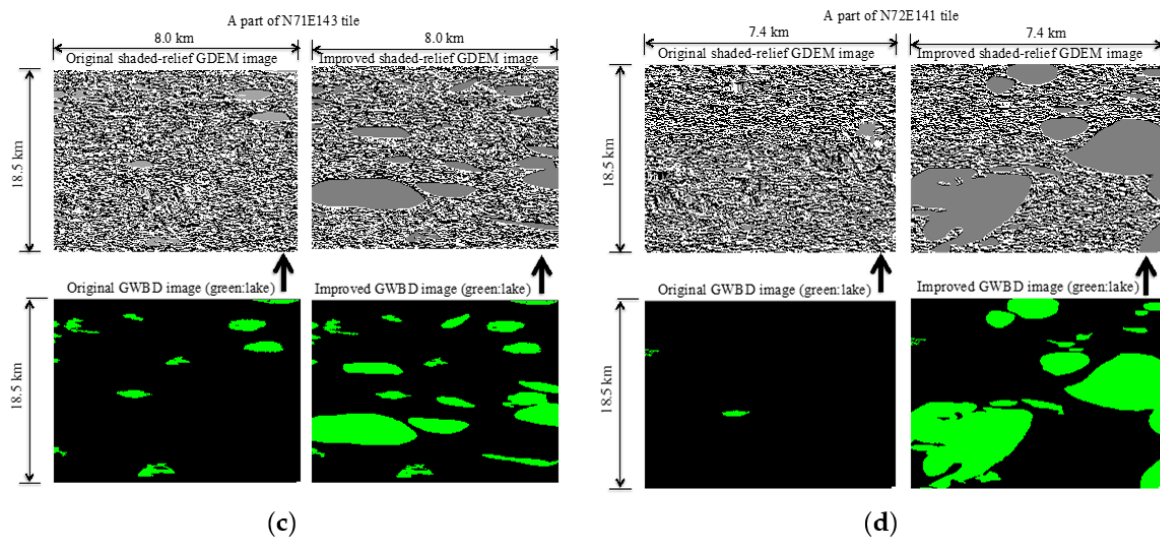
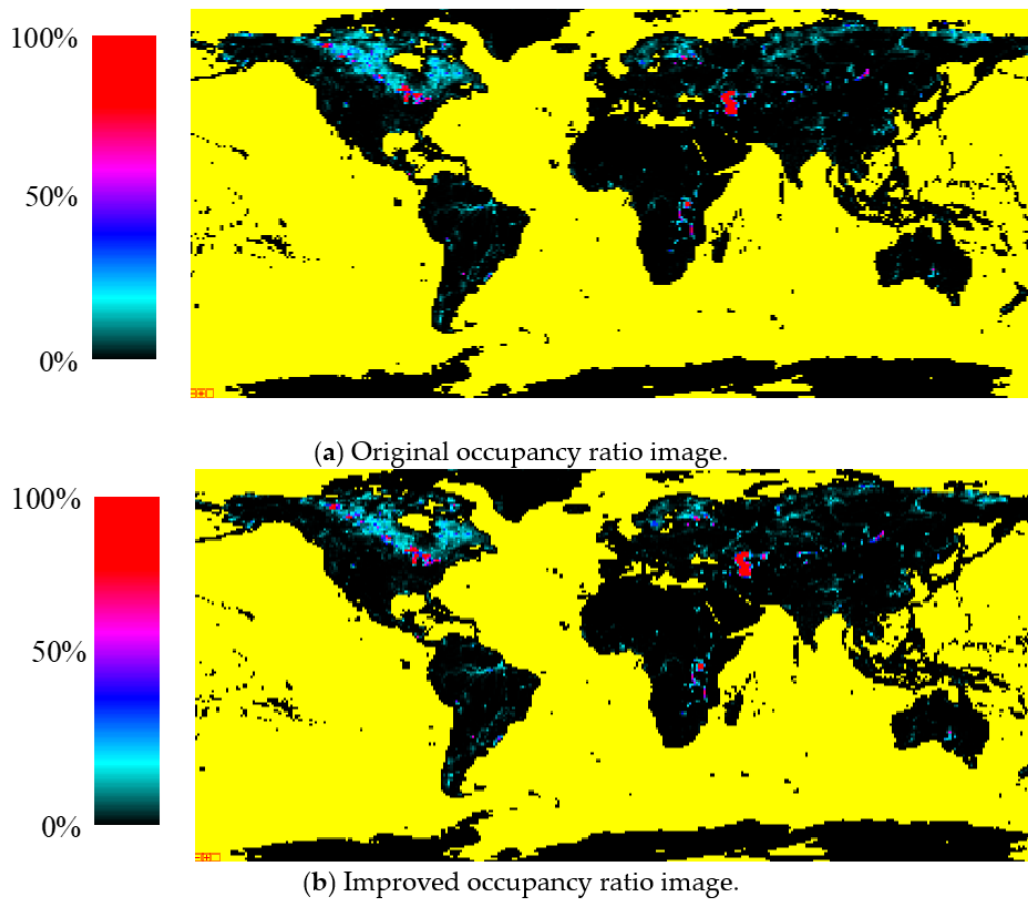


Figure 5. Cont.



**Figure 5.** Effect of improved GWBD to the corresponding GDEM. The two upper images are the original and improved shaded-relief GDEM images. The two lower images are the corresponding original and improved color density slice images. The green color denotes a lake water body, and the red color denotes a river water body: (a) a part of N60W076 tile images; (b) a part of N71E127 tile images; (c) a part of N71E143 tile images; (d) a part of N71E141 tile images.



**Figure 6.** Cont.

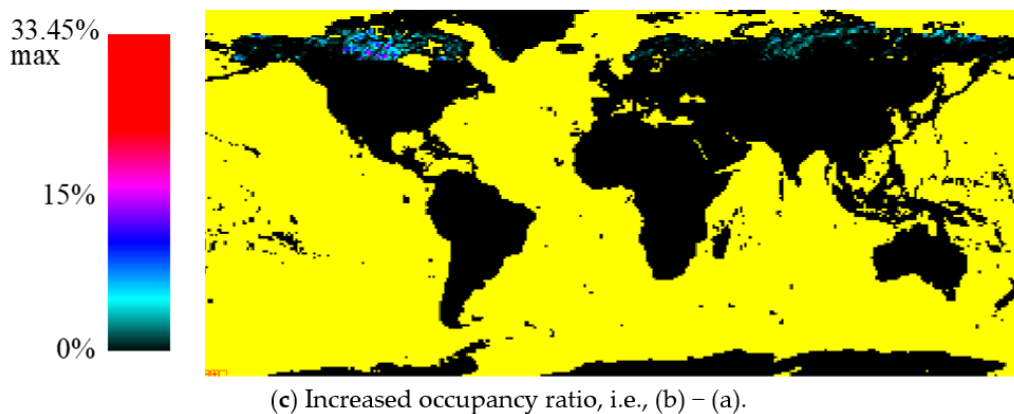


**Figure 6.** Global color density slice images of the improvement effect for the inland water body occupancy ratios. Large yellow-color areas denote sea areas. An inland water body means a lake or river: (a) Original occupancy ratio image; (b) Improved occupancy ratio image; (c) Increased occupancy ratio image.

Figure 6 is very useful to easily understand the various types of global outlines of inland water body distribution conditions. In addition to the global color density slice images of increased occupancy ratio, shown in Figure 6c, and which is main object of this paper, the global color density slice images of the improved occupancy ratio shown in Figure 6b give a complete global water body distribution with a  $1^\circ$  latitude by  $1^\circ$  longitude spatial resolution.

#### 4. Conclusions

Water body detection is an essential part of DEM generation, because image matching is not possible for water bodies. For inland water bodies like lakes and rivers, it is not possible to perfectly detect all water bodies using reflectance and spectral index, which are the only available parameters for optical sensor like ASTER. The only way available to identify the missed inland water bodies is to manually copy them with time-consuming visual inspection from the earth's surface images, like Landsat images. GeoCover2000 images are a main part of the reference images. CLAMS images are used to cover the deficiency of the GeoCover images. The water body improvement process is carried out mainly in the latitude of 60 degrees north and the further north areas, since the Shuttle Radar Topography Mission (SRTM) Water Body Data product (SWBD) [11] is available to make up undetected water body areas between south 56 degrees and north 60 degrees. South of south 56 degrees areas are not important for inland water bodies because of the frozen Antarctica. The original GWBD corresponds to ASTWBDV001, which was released to the public in August 2019 at the same time as ASTGTMV003 [12]. The ASTWBDV001 data are incorporated into ASTGTMV003. The improved correction was carried out using GeoCover and CLAMS as the reference data.

The improved GWBD almost completely covers all lake-type water bodies with an area greater than  $0.2 \text{ km}^2$ , and can be considered to be the final improvement. Further improvements for ASTER GDEM can be easily carried out by incorporating the improved GWBD into ASTGTMV003.

**Author Contributions:** Conceptualization, H.F.; methodology, H.F., M.U. and A.I.; investigation, H.F., M.U. and A.I.; writing—original draft preparation, H.F.; writing—review and editing, H.F., M.U. and A.I. All authors have read and agreed to the published version of the manuscript.

**Funding:** This research received no external funding.

**Acknowledgments:** We would like to acknowledge Japan Space Systems for supplying the ASTER data. The authors would also like to thank the ASTER Science Team members, specifically Level-1 and DEM Working Group members for their useful discussion. We also would like to acknowledge to National Institute of Advanced Industrial Science and Technology (AIST) for supplying original CLAMS data.

**Conflicts of Interest:** The authors declare no conflict of interest.

## References

1. Fujisada, H.; Sakuma, F.; Ono, A.; Kudos, M. Design and preflight performance of ASTER instrument protoflight model. *IEEE Trans. Geosci. Remote Sens.* **1999**, *36*, 1152–1160. [[CrossRef](#)]
2. Fujisada, H. ASTER Level-1 data processing algorithm. *IEEE Trans. Geosci. Remote Sens.* **1998**, *36*, 1101–1112. [[CrossRef](#)]
3. Fujisada, H.; Bailey, G.B.; Kelly, G.G.; Hara, S.; Abrams, M.J. ASTER DEM performance. *IEEE Trans. Geosci. Remote Sens.* **2005**, *43*, 2707–2714. [[CrossRef](#)]
4. Fujisada, H.; Iwasaki, A.; Hara, S. ASTER stereo system performance. *Proc. SPIE* **2001**, *4540*, 39–49.
5. Fujisada, H.; Urai, M.; Iwasaki, A. Advanced methodology for ASTER DEM generation. *IEEE Trans. Geosci. Remote Sens.* **2011**, *49*, 5080–5091. [[CrossRef](#)]
6. Fujisada, H.; Urai, M.; Iwasaki, A. Technical methodology for ASTER Global Water Body Data Base. *Remote Sens.* **2018**, *10*, 1860. [[CrossRef](#)]
7. GeoCover. Available online: [http://www.cr.chiba-u.jp/databases/GeoCover/TM\\_mosaic.html](http://www.cr.chiba-u.jp/databases/GeoCover/TM_mosaic.html) (accessed on 10 October 2020).
8. Gonzalez, L.; Valerie, V.; Yamamoto, H. Global 15-Meter Mosaic from Simulated True-Color ASTER Imagery. *Remote Sens.* **2019**, *11*, 441. [[CrossRef](#)]
9. Nelson, G.C.; Robertson, R.D. Comparing the GLC2000 and GeoCover LC land cover datasets for use in economic modelling of land use. *Int. J. Remote Sens.* **2007**, *28*, 4243–4266. [[CrossRef](#)]
10. Rajagopalan, R.; Aparajithan, S.; James, S.; Michael, C. Validation of Geometric Accuracy of Global Land Survey (GLS) 2000 Data. *Photogrammetric Eng. Remote Sens.* **2015**, *81*, 131–141.
11. NASA JPL. *NASA Shuttle Radar Topography Mission Water Body Data Shapefiles & Raster Files*; NASA EOSDISL and Processes DAAC: Sioux Falls, SD, USA, 2013.
12. Abrams, M.; Crippen, R.; Fujisada, H. ASTER Global Digital Elevation Model (GDEM) and ASTER Global Water Body Dataset (ASTWBD). *Remote Sens.* **2020**, *12*, 1156. [[CrossRef](#)]

**Publisher’s Note:** MDPI stays neutral with regard to jurisdictional claims in published maps and institutional affiliations.



© 2020 by the authors. Licensee MDPI, Basel, Switzerland. This article is an open access article distributed under the terms and conditions of the Creative Commons Attribution (CC BY) license (<http://creativecommons.org/licenses/by/4.0/>).